

# Experimental Investigation of Plane Jets Exiting Five Parallel Channels with Large Aspect Ratio

Laurentiu Moruz, Jens Kitzhofer, Mircea Dinulescu

**Abstract**—The paper aims to extend the knowledge about jet behavior and jet interaction between five plane unventilated jets with large aspect ratio (AR). The distance between the single plane jets is two times the channel height. The experimental investigation applies 2D Particle Image Velocimetry (PIV) and static pressure measurements. Our study focuses on the influence of two different outlet nozzle geometries (triangular shape with  $2 \times 7.5^\circ$  and blunt geometry) with respect to variation of Reynolds number from 5500 - 12000. It is shown that the outlet geometry has a major influence on the jet formation in terms of uniformity of velocity profiles downstream of the sudden expansion. Furthermore, we describe characteristic regions like converging region, merging region and combined region. The triangular outlet geometry generates most uniform velocity distributions in comparison to a blunt outlet nozzle geometry. The blunt outlet geometry shows an unstable behavior where the jets tend to attach to one side of the walls (ceiling) generating a large recirculation region on the opposite side. Static pressure measurements confirm the observation and indicate that the recirculation region is connected to larger pressure drop.

**Keywords**—2D particle image velocimetry, parallel jet interaction, pressure drop, sudden expansion.

## I. INTRODUCTION

MULTIPLE plane parallel jets have a large impact in many industrial applications like Plate-Type Heat Exchangers, Heating Ventilating and Air Conditioning systems (HVAC), drying systems as well as in combustion chambers. The target in most industrial applications is to have a low pressure drop when the jets expand into a larger cross section, a good mixing of the jets and to generate a uniform velocity distribution after a certain jet travelling length.

Single plane jets have been studied extensively since the pioneer works of [1]. Following studies mainly focused on characteristics of jet propagation and pointed out the importance and influence of initial boundary conditions, see e.g. [2]. Identified boundary conditions influencing the jet formation are Reynolds number based on nozzle gap height, nozzle AR, velocity profiles at exit including mean velocity profile as well as turbulence characteristics and nozzle geometry.

A systematical Reynolds number study from  $Re_h = 1500$  to 16500 for single plane jets has been performed more recently by [3], who tried to reduce influences of other initial boundary

Laurentiu Moruz is with the Apex Research B.V. - Apex Research Laboratory, Westeinde 10, 2275AD Voorburg, The Netherlands (phone: +31-(0)70-850-5786; e-mail: laurentiu.moruz@apexgroup.eu).

Jens Kitzhofer and Mircea Dinulescu are with the Apex Research B.V., Westeinde 10, 2275AD Voorburg, The Netherlands, (e-mail: jens.kitzhofer@apexgroup.eu, mircea.dinulescu@apexgroup.eu).

conditions. They found that jet formation in terms of mean velocity decay rate and evolution of turbulence intensity have a large impact up to  $Re_h = 10000$  and a reduced effect for  $Re_h > 10000$ .

Dual parallel jets have been studied by [4] and [5] beside others. An additional parameter defining the jet formation is the spacing between the jets. Here, two cases are defined, a ventilated and an unventilated case. The ventilated case has no wall between the jets, whereas in the unventilated case the jets are blocked by a wall. The further study in this paper concentrates on the unventilated case. Three main regions have been identified in literature, the converging region, the merging region, and the combined region. When the jets exit the nozzle, a recirculation zone with lower pressure is generated between the jets in the converging region. This low pressure region deflects the jets towards each other. The beginning of the merging region is defined by the merging point, where the recirculation zone vanishes, thus all streamwise velocities are positive. In the merging region the two jets merge together up to the combined point, where only a single combined jet can be identified.

Studies on multiple plane parallel jets are rare in literature. Multiple jets are mainly studied as round versions, e.g. in [6] and [7]. The authors mainly identify that the single jets merge and combine after a certain travel distance to one jet and that the outer jets are deflected towards the inner jet. A row of coplanar round jets has been studied by [8] more recently. Reference [8] applied latest measurement equipment like Laser Doppler Anemometry (LDA) and PIV and identified the importance of the consideration of coherent structures in the jet shear layers for the analysis of multiple parallel jets. Furthermore, he discussed the unstable behavior of the merging points and pointed statistical tools for the prediction of the jet behavior.

This paper is meant to set up experimental data including the definition of boundary conditions for multiple parallel plane jets exiting from different nozzle geometries. For that purpose, Chapter II describes the experimental set up, the applied measurement techniques like PIV and LDA and the measured boundary conditions upstream of the inlet into the five channel geometry as well as the boundary conditions exiting the channels at the nozzle outlet. The third chapter describes and discusses the experimental data with respect to mean velocity field and fluctuating velocity field in terms of Reynolds stress.

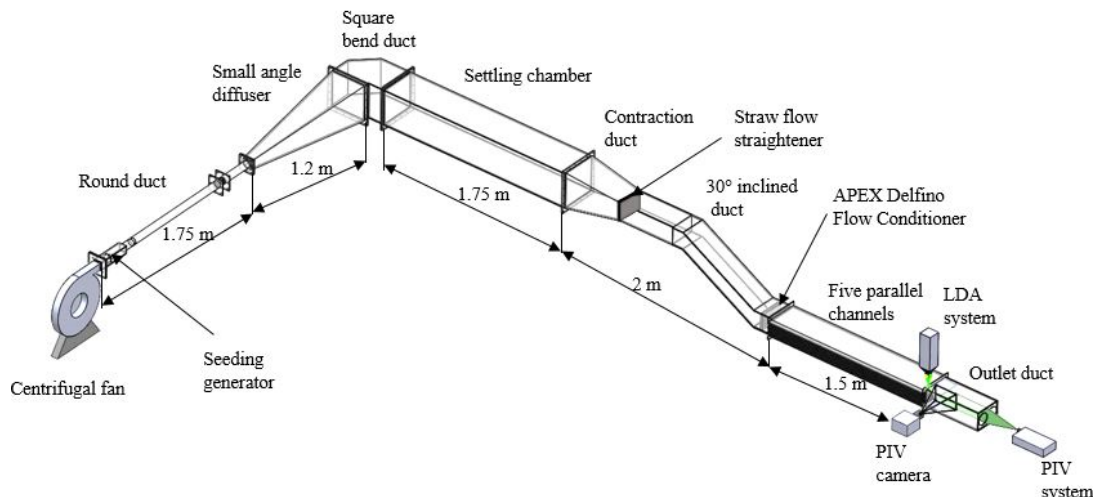


Fig. 1 Experimental Set-up for the analysis of the five parallel plane jets exiting the five channel geometry

## II. EXPERIMENTAL SETUP

### A. Overview Flow Facility

A transparent wind tunnel was designed to facilitate the air flow distribution in laminar, transient and turbulent regime upstream of the 5 plane parallel channels (see Fig. 1). A centrifugal fan with maximum volume flow rate of  $534 \text{ m}^3/\text{h}$  and 1.1 kW electric power accelerates the air through all the test facility. The volume flow rate is measured with a flow velocity probe from Testo installed at the aspiration side of the fan. To control the airflow, rate a digital variable power supply is used.

The air is transferred to the measurements position through a round duct, small angle diffuser, square bend, settling chamber, contraction duct,  $30^\circ$  inclined duct, Apex Delfino Flow Conditioner, five plane parallel channels, nozzle geometries and outlet duct.

The diffuser has a total angle of  $12^\circ$  for reducing the flow sidewall separation and the total pressure drop. The settling chamber has a squared section of  $0.3 \text{ m} \times 0.3 \text{ m}$  followed by a contraction duct with an AR of 1:3. The contraction duct is followed by a straws flow straightener of 50 mm length and straw diameter of 0.4 mm.

The ratio between the honeycomb cell diameter and length guarantees a removal of secondary flow like swirl.

The  $30^\circ$  inclined duct is used to facilitate a non-uniform flow profile just upstream of Apex Delfino Flow Conditioner, which consist of rectangular honeycomb structure and gradually changing fine mesh downstream of the honeycomb.

The five channel geometry consists of transparent plexiglass plates allowing optical measurement techniques. The channel height is  $h = 8 \text{ mm}$ , width is  $w = 200 \text{ mm}$  and the length is  $L = 1500 \text{ mm}$  (and hence a large AR of 25 between channel width/channel height). The non-dimensional spacing ratio between the channels is 2 and the contraction/expansion ratio at inlet/outlet is 3.5, velocity profile inside the channel is found to be turbulent for lower and higher Reynolds number (see Figs. 3 and 4). The Reynolds number is defined as:

$Re = u \times d_h / \mu$  where  $u$  is the mean velocity based on the volume flow rate,  $d_h$  is equivalent diameter of the channel which equals with  $2h$  and  $\mu$  is dynamic viscosity. The outlet geometry is varied between blunt geometry and triangular geometry. The dimensions can be found in Fig. 2. The length of triangular geometry is 60.77 mm with an angle of  $2 \times 7.5$  degrees.

### B. Overview of Measurement Equipment

The measurement techniques range from static pressure measurements to laser optical measurement techniques like PIV or LDA, see Fig. 5. For that purpose, a seeding generator introduces DEHS particles in the range of  $1 \mu\text{m}$  into the flow, immediately downstream of the fan.

LDA is applied to measure the upstream velocity profile in the center channel. The system is a 2D Flow Explorer from Dantec Dynamics. The LDA system is equipped with a 150 mm focal length lens generating a measurement volume of  $40 \mu\text{m}$  in diameter and  $200 \mu\text{m}$  in length. The system is traversed on an ISEL traverse with a positioning accuracy of  $\approx 7 \mu\text{m}$ . The analysis is performed in the BSA Flow Software. The stop criteria are defined with a measurement length of 30 s for each point, resulting in about 30000 samples or a data rate of 1000 bursts/s.

2D PIV is applied at the outlet duct to identify the topological behavior of the five parallel plane jets. The seeding particles are illuminated in the  $xz$ -plane at  $y=0.5 \text{ w}$  by a 145 mJ dual cavity laser equipped with a Dantec light sheet optics. The pulse length of the laser is 9 ns to avoid displacement of particles during the illumination. The scattered light of the particles is recorded by a double framing camera running at 10 Hz. The separation time between the images is adapted to the jets velocity to yield a maximum displacement of 10 Pixels. The number of double frames is 200 resulting in a measurement time of 20 s per geometry and Reynolds Number. The analysis of the particle images is performed in Dynamic Studio with the "Adaptive PIV" routine. The Cross Correlation algorithm automatically

chooses an interrogation area size with respect to number of particles. The minimum number of particles is chosen to be 6/interrogation area. For increased accuracy in shear flows, the algorithm deforms the interrogation area to cover rotation,

tension and shear. Erroneous vectors are detected by the universal outlier detection method. The scaling is 12 Pixels/mm. The resulting vector field has a vector pitch of 16 Pixels (1.3/mm).

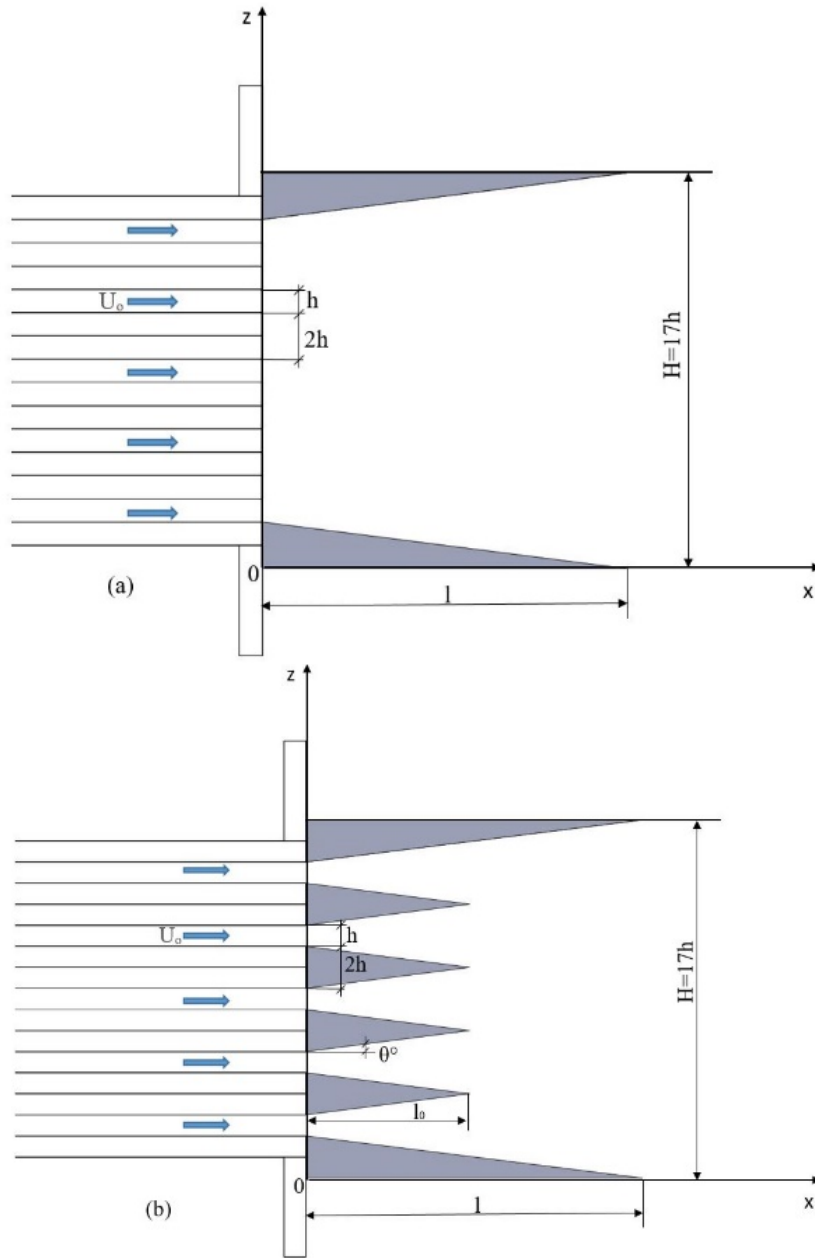


Fig. 2 (a) Blunt geometry, (b) triangular geometry

### C.Inlet Flow Conditions

As stated in literature, the analysis of multiple jets is very sensitive to inlet and boundary flow conditions. Thus, the exact knowledge of those conditions is necessary. Figs. 3 and 4 show the velocity profiles and fluctuating velocity profiles in the symmetry plane 3h upstream of the inlet into the five channel geometry measured with PIV. Due to the 30° turn, the

velocity profile is unsymmetrical and has maximum fluctuations of about 10% of the mean velocity. The installation of the Apex Delfino Flow Conditioner makes the velocity profile more uniform and reduces the fluctuations to about 3%.

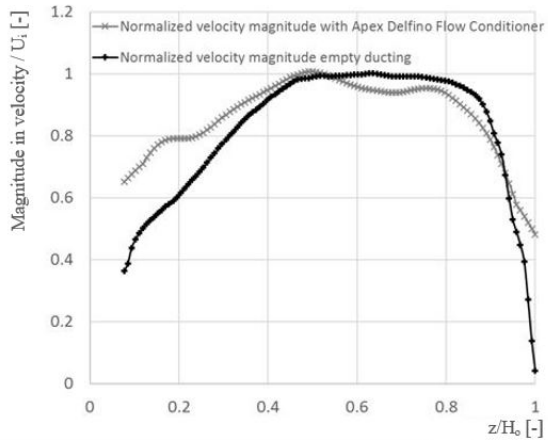


Fig. 3 Normalized Velocity profile (with maximum cross sectional velocity in x-direction) at a stream wise position 5 h upstream of the inlet into the five channel model with and without Flow Conditioner (installed immediately downstream of the 30 degree ducting)

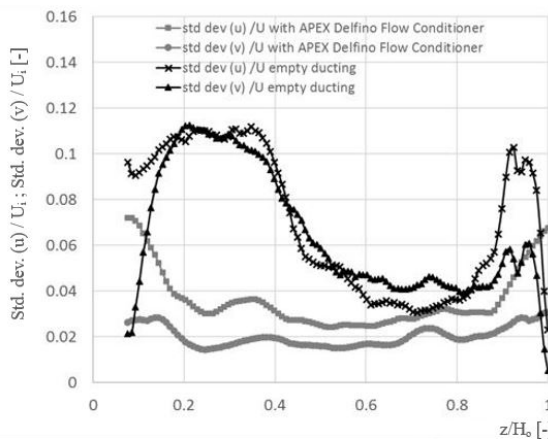


Fig. 4 Profile of normalized standard deviation (normalized with maximum cross sectional velocity in x-direction) at a stream wise position 5h upstream of the inlet into the five channel model with and without Flow Conditioner (installed immediately downstream of the 30 degree ducting)

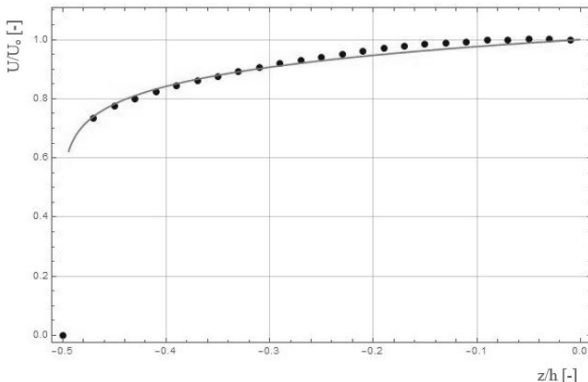


Fig. 5 (dots) Normalized velocity profile in the center channel 5h upstream of the nozzle outlet measured with LDA, (line) Least Squares Fit of turbulent velocity profile with  $m=0.9$

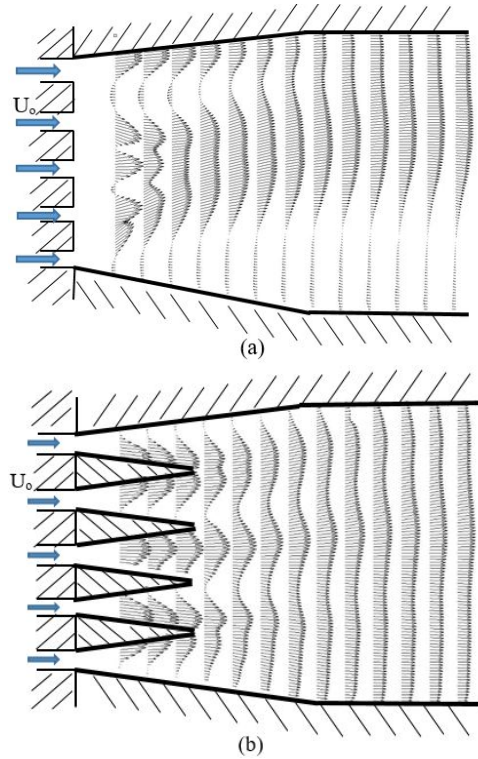


Fig. 6 Mean velocity distribution in the symmetry plane at  $y/w = 0.5$  for the blunt geometry (a) and the triangle geometry (b) visualized with vectors

The velocity profile inside the channels is representatively shown in Fig. 5 for the center channel about 5h upstream of the nozzle outlet for a Reynolds number of 5500. The corresponding mean factor  $m$  for turbulent velocity profiles is calculated by least square curve fitting and equals to  $m=0.9$  confirming the turbulent character of the outlet velocity.

### III. RESULTS AND DISCUSSION

#### A. Mean Velocity Field

Fig. 6 shows the global mean velocity field downstream of the nozzle exit visualized with vector profiles for the blunt and the triangular geometry.

For the blunt geometry, the top jet tends to move along the top wall, whereas the 4 bottom jets merge together in a rather short distance ( $x/h = 4 - 5$ ). The combined jets are then directed towards the strong wall jet, which as a result generates a large recirculation zone on the bottom of the outlet duct. At a position far downstream of the outlet nozzles all jets are merged together and the position of the combined jet is in the upper half of the duct resulting in an asymmetrical velocity profile at  $x/h > 15$ .

The triangular geometry shows a more symmetrical behavior. Smaller recirculation zones are generated on the top and bottom angle wall. The two top and bottom jets merge together immediately downstream of the sharp trailing edge of the triangular geometry. The center jet seems to be unaffected

of the combined top and bottom jets. The top and bottom jets combine further downstream and start to merge together with the center jet. In comparison with the blunt geometry, no large recirculation zone is formed on the bottom wall resulting in a uniform velocity profile at  $x/h > 15$ .

The normalized velocity profiles at the merging points of the jets are shown in Fig. 7 for the blunt geometry. The merging point is defined at the position where the velocity between the jets is 0. The 5 jets are clearly visible at  $x/h=4$ . The two bottom jets already started to merge together, whereas the merging points of jets 3 and 4 is at  $x/h=4$ . At

$x/h=5$  jets 1 and 2 are in the combining process as well as jets 3 and 4. The wall jet remains at the wall. At  $x/h=9$ , all 4 jets are combined and the combined jets start to merge with the wall jet.

Fig. 8 shows the normalized velocity profile in the far field at position  $x/h=20$  for the two investigated Reynolds numbers. The asymmetric profile is clearly visible, which is a result of the 4 combined jets that merge with the wall jet. For both Reynolds numbers, the normalized velocity profiles are nearly overlapping.

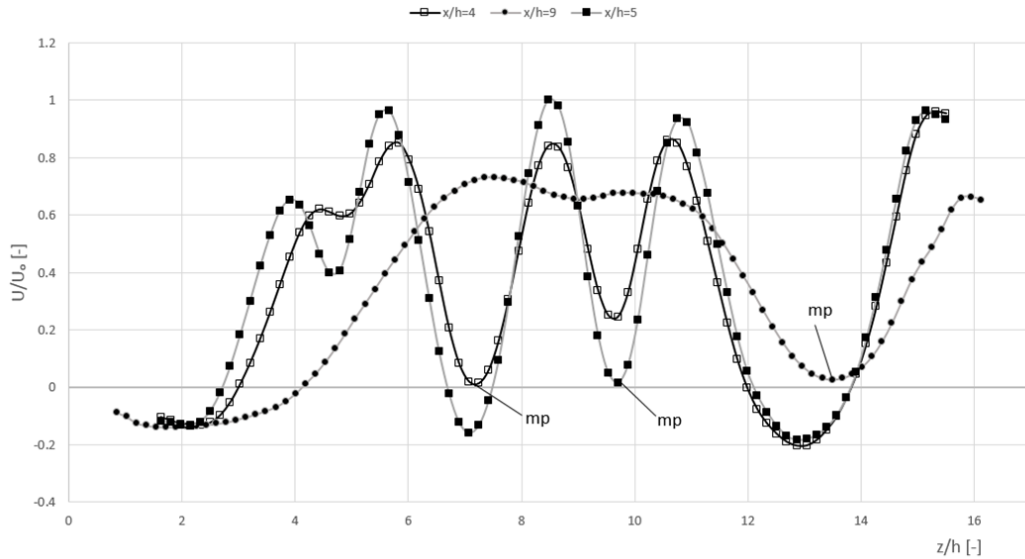


Fig. 7 Normalized mean velocity profiles as function of  $z/h$  at positions defined by three observable merging points (mp) for the blunt geometry at  $Re=12000$

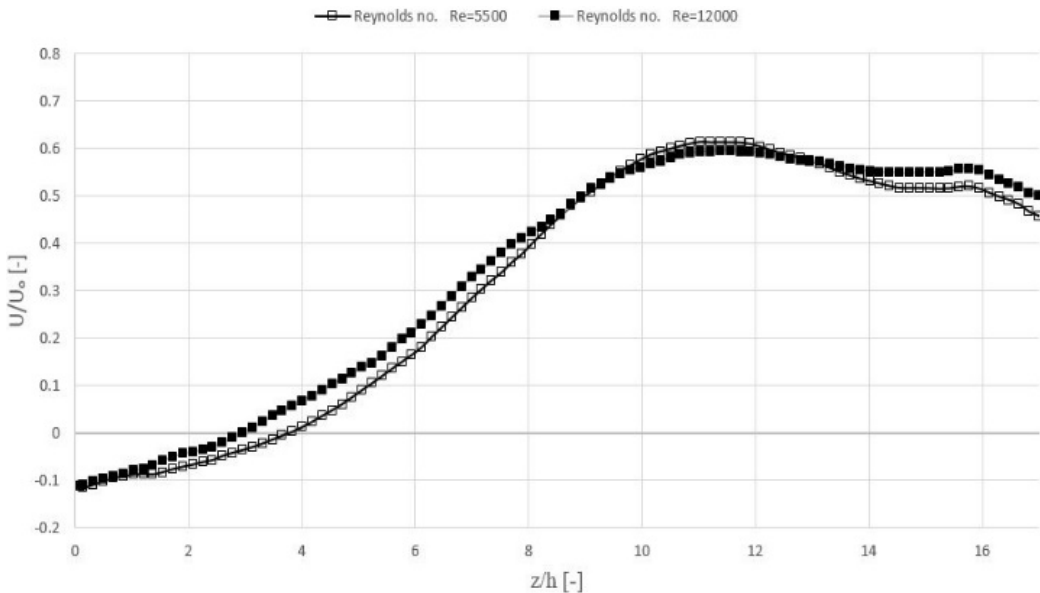


Fig. 8 Normalized mean velocity profiles as function of  $z/h$  at  $x/h=20$  for the blunt geometry at different Reynolds numbers

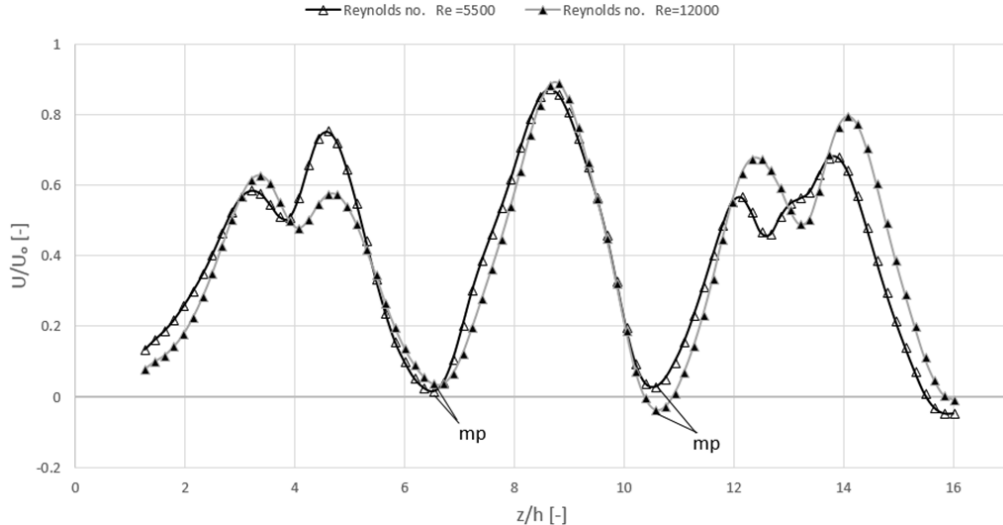


Fig. 9 Normalized mean velocity profiles as function of  $z/h$  at positions defined by two observable merging points (mp) for the triangular geometry at different Reynolds numbers

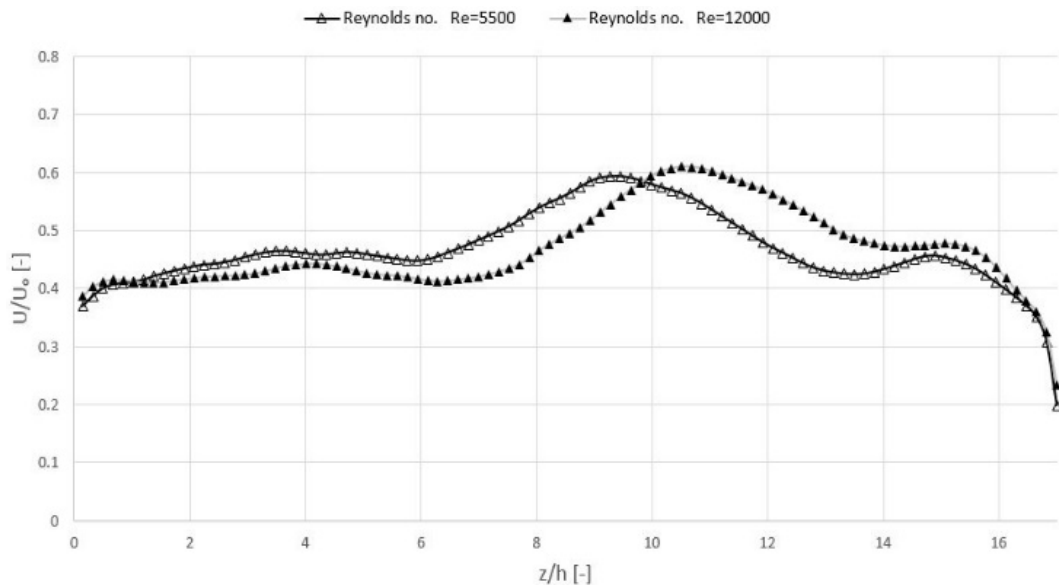


Fig. 10 Normalized mean velocity profiles as function of  $z/h$  at  $x/h=20$  for the triangular geometry at different Reynolds numbers

The normalized velocity profiles for the triangular geometry at the position of the first observable merging points ( $x/h=5$ ) is shown in Fig. 9 and the profiles in the far field at the position  $x/h=20$  is shown in Fig. 10. At  $x/h=5$  the two upper and lower jets have already merged, but it is still possible to discriminate the single jets. The center jet shows highest velocities, thus trying to pull the outer jets. A wall jet is not observable as in the case of the blunt geometry. In the far field at  $x/h=20$  all jets are nearly combined and build a rather uniform velocity distribution over the complete cross section.

#### B. Reynolds Stress

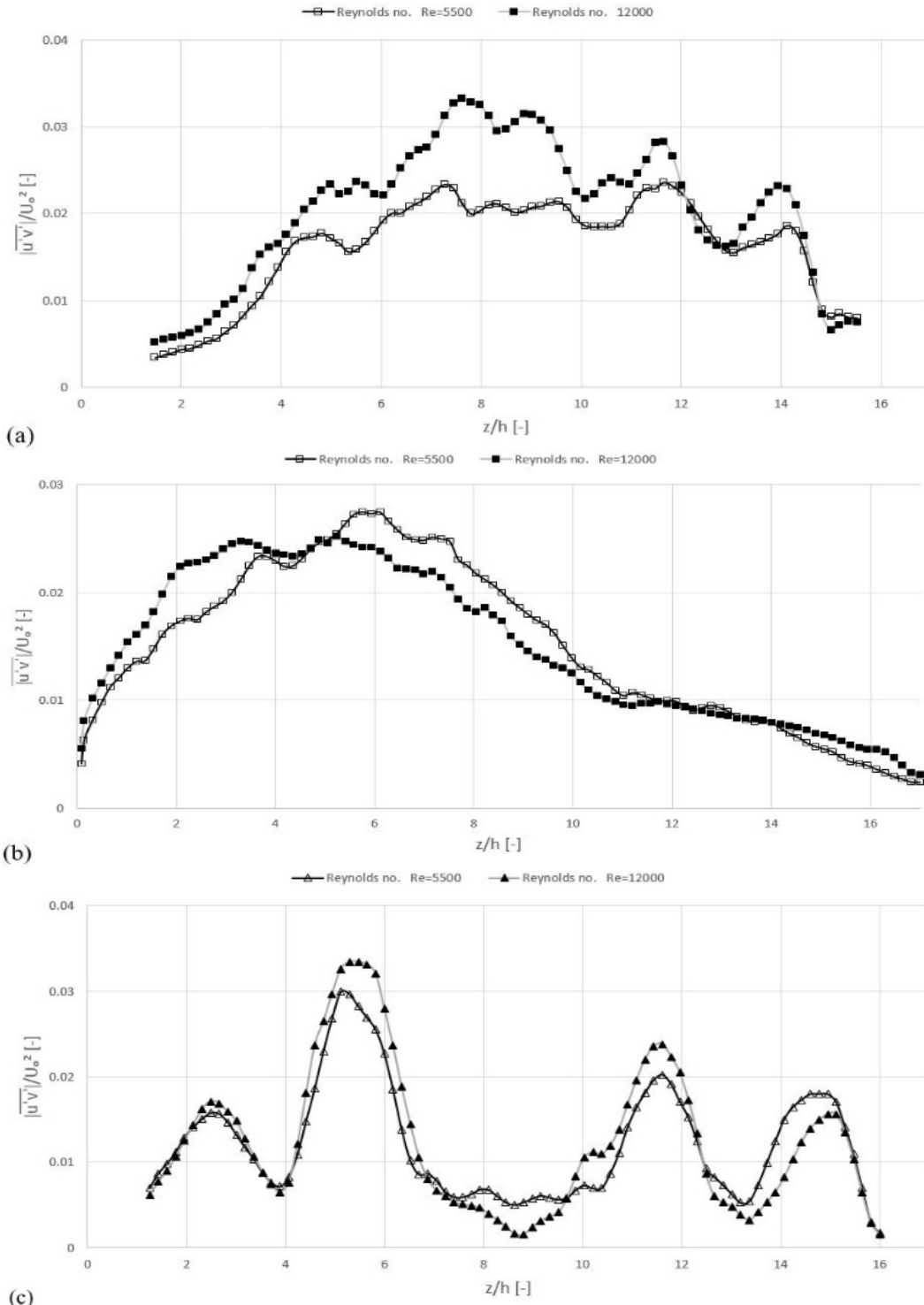
The Reynolds stress can be understood as an indication for the amount of mixing of a fluid. A velocity field can be decomposed in a mean velocity field and a fluctuating velocity

field. Both are indirectly delivered by 2D PIV measurements. The mean velocity field is calculated by summing up the 200 instantaneous velocity field. The fluctuating velocity field is then calculated by subtracting the mean velocity field from the instantaneous ones. Both fluctuating velocity components in  $x$  and  $z$  direction,  $u'$  and  $v'$ , are then multiplied and averaged over all 200 time steps. To have a measure of the strength in mixing, the normalized magnitude of Reynolds stress is shown in Fig. 11 for the blunt and triangular geometry at positions of the merging points and in the far field at  $x/h=20$ .

At the position of the merging points, the normalized Reynold stress shows a rather flat profile with a mean normalized Reynolds stress of 0.025, with decreasing values close to the top and bottom walls. The two upper and the two

lower jets, for the triangular geometry, are already in the combining region and the center jet seems to be unaffected. Beside the peaks at positions where the upper and lower jets combine, the level of Reynold stress is below 0.01, which is more than half of the corresponding Reynold stress of the

blunt geometry. The same statement holds for the far field at position  $x/h=20$ , where the Reynolds stress for the blunt geometry is about 2-3 times larger than for the triangular geometry.



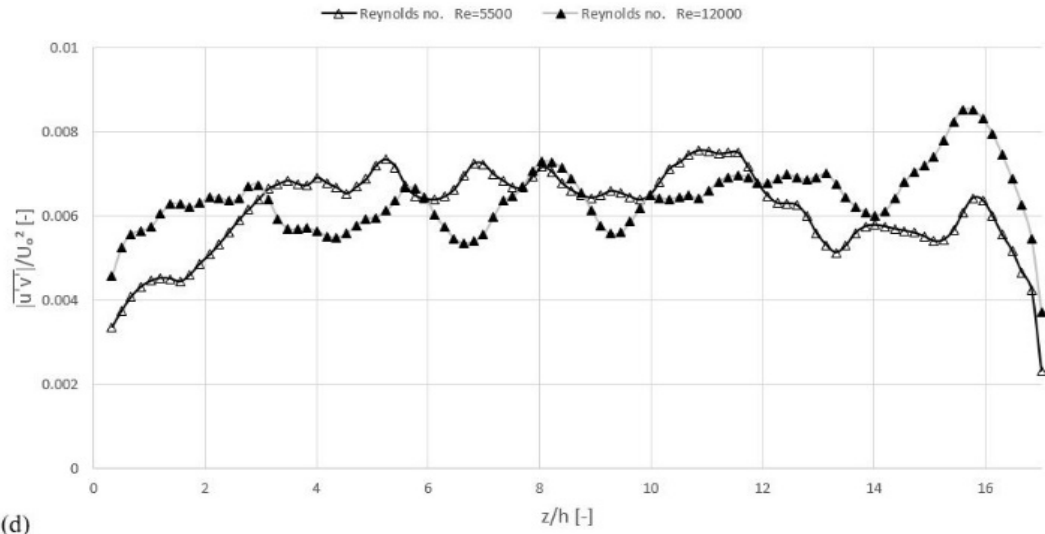


Fig. 11 Normalized Reynolds stress for (a) blunt geometry at position of merging points, (b) blunt geometry at position  $x/h=20$ , (c) triangular geometry at position of merging points, (d) triangular geometry at position  $x/h=20$

#### IV. CONCLUSION

The blunt geometry shows an unsymmetrical velocity profile due to the wall jet and the recirculation zone.

The triangular geometry generates a smooth expansion into the outlet duct (measurement field). The recirculation zones, in this case, appear due to merging of side jets (the first two jets close to the top and last two jets close to the bottom).

The large Reynolds stress of the blunt geometry indicates strong mixing in comparison with lower Reynolds stress of the triangular geometry.

Laser Optical Measurement equipment is well suited for the analysis of such complicated velocity fields as multiple interacting jets.

#### REFERENCES

- [1] H. Schlichting, "Laminare Strahlausbreitung", in *ZAMM* 13, 260, 1933
- [2] R.C. Deo, "Experimental investigations of the influence of Reynolds number and boundary conditions on a plane air jet", *PhD. thesis*, University of Adelaide, Australia, 2005
- [3] Ravinesh C. Deo et al., "The influence of Reynolds number on a plane jet", in *Physics of Fluids* 20, 075108, 2008
- [4] Miller, D.R., Comings, E.W. (1960), "Force-momentum fields in a dual-jet flow", in *Journal of Fluid Mechanics* 7 (2), 237-256, 1960
- [5] Nasr, A., Lai, J.C.S., "The effects of nozzle spacing on the development of two parallel plane jets", in *International Journal of Transport Phenomena* 2 (1), pp. 57-70, 2000
- [6] Cho, Y., Awbi, H.B., Karimipanah, T., "Theoretical and experimental investigation of wall confluent jets ventilation and comparison with wall displacement ventilation", *Building and Environment* 43 (6), pp. 1091-1100, 2008
- [7] Corrsin, S., "Investigation of the behavior of parallel two-dimensional air jets", NASA No. 4H24, 1944
- [8] Ghahremanian, S., A near-field study of multiple interacting jets: Confluent jets, *PhD. thesis*, Linköping University, Institute of Technology, Sweden, 2014